Sigma J Eng Nat Sci, Vol. 42, No. 1, pp. 211–224, February, 2024

Sigma Journal of Engineering and Natural Sciences
Web page info: https://sigma.yildiz.edu.tr
DOI: 10.14744/sigma.2024.00018

Research Article

Prediction of inelastic displacement ratios for evaluation of degrading SDOF systems: A comparison of the scaled conjugate gradient and Bayesian regularized artificial neural network modeling

Muzaffer BÖREKÇİ[1,*], Burak AYDOĞAN[2]

[1]*Department of Civil Engineering, Yildiz Technical University, Istanbul, 34220, Türkiye*
[2]*Department of Civil Engineering, Gebze Technical University, Kocaeli, 41400, Türkiye*

ARTICLE INFO

Article history
Received: 30 January 2022
Revised: 05 April 2022
Accepted: 20 June 2022

Keywords:
Artificial Neural Network; Degradation; Dynamic Instability; Inelastic Displacement Ratio; Nonlinear Regression Analysis; Nonlinear Time History Analysis

ABSTRACT

Inelastic displacement demand is an important part of the performance-based design and it should be estimated realistically to determine a reliable seismic performance of a structure. In this context, the coefficient method is an easy and practical method for this estimation. The coefficient method is a method that is used to estimate inelastic displacement demand by the multiplication of the elastic displacement demand and inelastic displacement ratio. Thus, it is clear that a reliable estimation of inelastic displacement demand depends on a reliable inelastic displacement ratio. After a reliable estimation of the inelastic displacement ratio, it is essential to propose an equation for the usage of engineering practice. Although nonlinear regression analysis is preferred in the literature as a classical method to estimate an equation, the Artificial Neural Network method is a new and modern way that can be used in the estimation of inelastic displacement ratio. In this study, Artificial Neural Network models have been proposed by using data of inelastic displacement ratios of Single Degree of Freedom systems with stiffness and strength degrading peak-oriented hysteretic model and collapse potential by performing nonlinear time history analyses. Firstly, a large number of trials have been conducted to obtain an optimum Artificial Neural Network model. The results of Artificial Neural Network models have been compared to the results of equation estimated by using nonlinear regression analysis and given in the previous studies. According to the results, Artificial Neural Network models give closer values to the inelastic displacement ratios of time history analysis than nonlinear regression analysis. Especially, the Bayesian Regularization Backpropagation model of the Artificial Neural Network method with two hidden layers achieved the best performance among the other Artificial Neural Network models. It can be said that Artificial Neural Network methods can be used to estimate inelastic displacement ratio since it yields better accuracy than previous techniques for different parameters.

Cite this article as: Börekçi M, Aydoğan B. Prediction of inelastic displacement ratios for evaluation of degrading SDOF systems: A comparison of the scaled conjugate gradient and Bayesian regularized artificial neural network modeling. Sigma J Eng Nat Sci 2024;42(1):211–224.

***Corresponding author.**
*E-mail address: mborekci@yildiz.edu.tr

This paper was recommended for publication in revised form by Regional Editor Ahmet Selim Dalkilic

Published by Yıldız Technical University Press, İstanbul, Turkey

INTRODUCTION

Structures behave nonlinearly and may suffer heavy damage under the effect of a severe earthquake. It is well-known from past studies that damages to structures under the effect of a severe earthquake occur because of the large displacement instead of strength. Thus, it is important to determine the seismic displacement demand of a structure accurately.

Although nonlinear time history analysis is the most reliable method, it is still not practical and requires a significant amount of run-time to determine the inelastic displacement demand. Thus, more straightforward methods are still needed to estimate the desired inelastic displacement demand. (IDD)

Among the several methods, using "inelastic displacement ratio" (IDR) is one of the effective one in the estimation of IDD. IDR is the ratio of inelastic and elastic displacement demand and using this method is a very simple and practical way to estimate the IDD. In this method, IDD is estimated by multiplying the elastic displacement demand of the corresponding system with IDR. Many researchers studied IDR and proposed equations for different structural systems and hysteretic behaviors.

Veletsos and Newmark [1] were the first researchers to study the relationship between inelastic and elastic displacement demand. They observed that the deformation of elastic and inelastic Single Degree of Freedom (SDOF) systems are very close for long periods using three earthquake ground motions, based on the elastic-perfectly plastic behavior. This observation is the "equal displacement rule". According to their study, inelastic deformation demand is higher than the elastic deformation demand for short-period SDOF systems.

Shimazaki and Sozen [2] investigated the elastic and inelastic displacement demand of SDOF systems using the El-Centro ground motion record and confirmed the "equal displacement rule" for periods longer than the characteristic period. IDD is higher than the elastic displacement demand for periods shorter than the characteristic period and the difference between the inelastic and elastic displacement demands depends on the considered hysteretic models. Qi and Moehle [3] confirmed the conclusions of the study of Shimazaki and Sozen [2].

Miranda [4-6] studied IDR and gave important results on IDR in the short period region and investigated the limiting periods of the spectral regions where the equal displacement rule is applicable.

Miranda [7], Ruiz-Garcia and Miranda [8], Vidic et al. [9], Aydinoglu and Kaçmaz [10], Chopra and Chintanapakdee [11], and Eser et al. [12] investigated IDR and proposed equation based on non-degrading bilinear hysteretic behavior. Durucan and Durucan [13] investigated IDR and proposed an equation based on non-degrading bilinear hysteretic behavior. Zhai et al. [14] investigated IDR for structures with constant damage performance using no pulse-like ground motions for non-degrading elastoplastic systems. Wen et al. [15] conducted the same study as Zhai et al. [14] unlikely using near-fault pulse-like ground motions.

Studies showed that structures deteriorate under the effect of cycling loadings [16]. Also, it is well-known that the hysteretic behavior of RC buildings is not similar to the bilinear hysteretic behavior, on the contrary, it is similar to peak-oriented hysteretic behavior and has strength and stiffness degradation [17, 18]. It is important to estimate a reliable IDR equation to determine an approximate seismic performance and for this purpose, a realistic hysteretic behavior should be considered in the estimation of IDR. Chintanapakdee and Jaiyong [19] demonstrated that the displacement time history of Single Degree of Freedom (SDOF) systems closely approximates the roof displacement of corresponding Multi Degree of Freedom (MDOF) reinforced concrete (RC) moment-resisting frames when utilizing a degrading peak-oriented hysteretic model, as opposed to a non-degrading bilinear hysteretic model.

Nassar and Krawinkler [20], Rahnama and Krawinkler [21], and Seneviratna and Krawinkler [22] investigated IDD and proposed equations of IDR for different hysteretic behavior considering strength degradation, stiffness deterioration, and pinching effect. However, strength degradation, stiffness deterioration, and pinching effect were considered separately in the estimation of IDR. It is well-known that these effects may occur simultaneously or affect each other.

Gupta and Kunnath [23] investigated the effect of hysteretic model parameters on IDD based on the three-parameter strength degradation hysteretic model.

Song and Pincheira [24] conducted a study on IDD based on stiffness and strength degrading systems. According to their study, the IDD of degrading systems can be higher than those of non-degrading ones. Pekoz and Pincheira [25] studied IDR considering the same hysteretic model given in the study of Song and Pincheira [24]. According to their study, the IDD of degrading systems is larger than the IDD of non-degrading systems for periods shorter than the characteristic period of ground motion.

Chenouda and Ayoub [26] investigated IDD based on bilinear and Clough hysteretic models with stiffness and strength degradation considering collapse potential. The hysteretic models they considered in their study are energy-based models and more realistic for RC structures. Also, they modified the equations of IDR proposed by Nassar and Krawinkler [20] and Chopra and Chintanapakdee [11]. Although the hysteretic model, which Chenouda and Ayoub [26] considered in their study, is more realistic, they considered limited degradation cases in the estimation of equations.

Lumantharna et al. [27] investigated the effect of the degradation on IDD of ground motions with different characteristic periods and they concluded that the degradation

effect on IDD becomes significant with the longer characteristic period.

Borekci et al. [28] investigated the effect of the hysteretic model and degradation on IDD and proposed an equation of IDR for SDOF systems with constant lateral strength considering an energy-based stiffness and strength degrading peak-oriented hysteretic model with collapse potential. Also, they considered possible degradation cases in the estimation of IDR. According to the result of this study, the non-degrading bilinear hysteretic model gives a lower IDR than the degrading peak-oriented hysteretic model.

As it is stated above, a reliable estimation of IDR is very important in the determination of the seismic performance of a structure. Considered hysteretic behavior is an important key in the estimation of IDR and an energy-based stiffness and strength degrading peak-oriented hysteretic model with collapse potential gives more realistic IDR for RC buildings. After the estimation of IDR with the conduction of time history analysis, an appropriate equation should be given. Former studies used nonlinear regression analysis to propose the equation of IDR. However, an artificial neural network (ANN) is a new and modern method that can be used in the estimation of IDR for more accurate results. Xie et al. [29] conducted a detailed study that is a review of the application of machine learning (ML) including ANN in earthquake engineering. The study examines four main topic areas of ML implementations including seismic hazard analysis, system identification and damage control, seismic fragility assessment, and structural control for earthquake mitigation. Xi et al. [29] indicate that the implementation of ML in earthquake engineering is still in its early stage when compared with other disciplines. Dwairi and Tarawneh [30] conducted a study to predict IDR by using ANN. Dwairi and Tarawneh [30] have predicted the IDR of SDOF systems built on soft soils for constant ductility by considering 4 hysteretic models as Flag-shaped, Small Takeda, Large Takeda, and Elastic-perfectly plastic systems. While Flag-shaped and Elastic-perfectly plastic models are non-degraded, the other two consider only ductility-based stiffness degradation. The selected input parameters for ANN are only ductility and the ratio of the fundamental periods of structure and ground motion. According to their study, predictions of IDR using ANN show high accuracy and low mean square error (MSE), when compared to those estimated by using nonlinear regression analysis, and this result confirms the result of the current study. Wei et al. [31] conducted comprehensive research on the effects of various structural and ground motion parameters on the residual displacement of non-degraded bilinear SDOF systems under near-fault ground motion records and proposed a prediction by implementing ANN with the Backpropagation model. They stated that ANN has good accuracy in predicting the residual displacements of SDOF systems.

Although ANN has a complex procedure for the estimation of reliable results, it is useful in predicting with high correlation in case of the complex relationships between variables. However, despite its complex procedure, it is relatively easy to determine an output value by using a proper computer program that runs the proposed ANN training.

In this study, IDR equations are estimated for SDOF systems using ANN methods with two different models Scaled Conjugate Gradient (SCG) and Bayesian Regularization Backpropagation (BRB). Results of ANN methods were compared with the nonlinear regression analysis results given in the study of Borekci et al. [28]. IDR data were taken from the study of Borekci et al. [28] and the data were computed for a set of 53 natural vibration periods ranging from T = 0.1 s. to T = 3 s. (T = 0.1:0.02:0.2, 0.22:0.03:1, 1.1:0.1:3), 6 strength reduction factors (R_y =1.5, 2, 3, 4, 5, 6), 3 post-yield stiffness ratios (α_s = 0%, 3%, 5%) and 160 ground motion records and 27 different combinations of degradation. 4121280 time history analyses were conducted to estimate IDR. While the considered hysteretic model and its parameters have been stated in Section 2, knowledge about the ground motion records and selection parameters has been given in Section 3. The estimation procedure of IDR and details of the ANN method have been comprehensively explained in Sections 4 and 5, respectively. Results of the ANN method and comparison of the ANN method and nonlinear regression solutions have been given in Section 6. ANN methods, especially the BRB model, proved to be a better estimator for IDR than the methods already available in the literature. The presented ANN model is fast, accurate, and easy to use on any PC.

HYSTERETIC MODEL AND PARAMETERS

Experimental investigations revealed that the behavior of RC buildings or components subjected to cyclic loading deviates from the bilinear hysteretic response, with stiffness-strength degradation persisting throughout the cyclic loading process [17]. Degradation has a significant effect on IDR, especially in the short period region of the response spectrum [24, 25, 27, 28]. Thus, the stiffness and strength degrading peak-oriented hysteretic model should be considered to estimate a reliable IDR of RC buildings. For this purpose, an energy-based stiffness and strength degrading peak-oriented hysteretic (SSDPH) model with the collapse potential is considered in this study. This model adheres to the fundamental hysteretic rules proposed by Clough and Johnston [32], later modified by Mahin and Bertero [33]. However, the backbone curve has been adjusted by Ibarra et al. [16] to incorporate strength capping and residual strength, as illustrated in Figure 1 [16]. In Figure 1, f_r represents the residual strength, f_c is the maximum strength, u_c denotes the cap displacement at the onset of the softening branch, and K_c represents the post-capping stiffness, typically with a negative value. An example of SSDPH cycling is illustrated in Figure 2. For further details, refer to the study by Ibarra et al. [16].

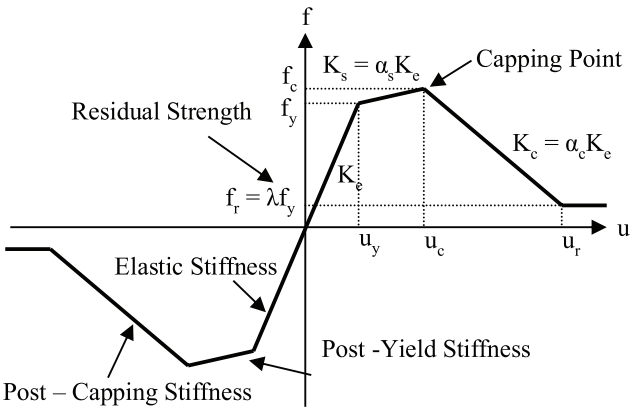

Figure 1. Backbone curve of Peak-Oriented hysteretic behavior [16].

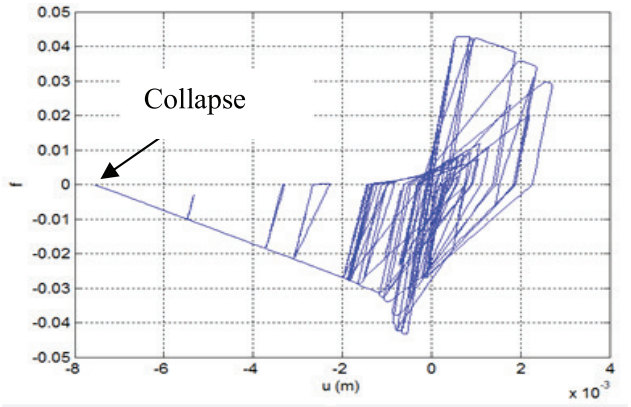

Figure 2. An example for a hysteretic behavior with cyclic degradation and collapse.

Ibarra et al. [16] proposed three degradation parameters: γ, u_c/u_y, and αc. γ denotes the rate of deterioration, with faster deterioration associated with decreasing values of γ. For instance, γ = 50, γ = 100, and γ = 150 correspond to severe, moderate, and low degradation systems, respectively [26]. u_c/u_y represents the ratio between the displacement at peak strength and yield strength. The considered ratios of u_c/u_y are 2, 4, and 6, where these values signify non-ductile, medium ductile, and very ductile structures, respectively [34]. α_c is utilized to define the post-capping stiffness ratio and is characterized by negative values. The values of αc include -6% [26], -14%, and -21% [35], representing small, medium, and large slopes, respectively. In this study, the medium slope is assumed to be -14%.

In this study, two collapse criteria were considered: dynamic instability and energy exhaustion. As is seen in Figure 2, once the post-capping branch reaches the horizontal axis, dynamic instability, accordingly, collapse occurs [16, 26, 35, 36]. If a slight increase in the input's intensity leads to minor alterations in the response, the structure undergoing this input is considered stable [37, 38]. In other words, when the post-capping branch intersects the horizontal axis, the stiffness of the system becomes zero, and this situation causes huge and erroneous responses in the solution. Otherwise, the structure will not be stable and it is called dynamic instability. The second assumption is the energy-based collapse and if hysteretic energy capacity is exhausted, the system collapses. In this study, reaching the hysteretic energy dissipation capacity is the second criterion for the collapse in addition to the dynamic instability. Degradation occurs with the combination of degradation parameters (γ, u_c/u_y, α_c), and all the combinations considered within the scope of this study are given in Table 1.

Table 1. Considered combinations of deterioration parameters

Name	γ	αc	uc/uy	Name	γ	αc	uc/uy
γ50_α_c6_u_c/u_y2	50	-6%	2	γ100_α_c14_u_c/u_y6	100	-14%	6
γ50_α_c6_u_c/u_y4	50	-6%	4	γ100_α_c21_u_c/u_y2	100	-21%	2
γ50_ α_c6_u_c/u_y6	50	-6%	6	γ100_α_c21_u_c/u_y4	100	-21%	4
γ50_α_c14_u_c/u_y2	50	-14%	2	γ100_α_c21_u_c/u_y6	100	-21%	6
γ50_α_c14_u_c/u_y4	50	-14%	4	γ150_α_c6_u_c/u_y2	150	-6%	2
γ50_α_c14_u_c/u_y6	50	-14%	6	γ150_α_c6_u_c/u_y4	150	-6%	4
γ50_α_c21_u_c/u_y2	50	-21%	2	γ150_α_c6_u_c/u_y6	150	-6%	6
γ50_α_c21_u_c/u_y4	50	-21%	4	γ150_α_c14_u_c/u_y2	150	-14%	2
γ50_α_c21_u_c/u_y6	50	-21%	6	γ150_α_c14_u_c/u_y4	150	-14%	4
γ100_α_c6_u_c/u_y2	100	-6%	2	γ150_α_c14_u_c/u_y6	150	-14%	6
γ100_α_c6_u_c/u_y4	100	-6%	4	γ150_α_c21_u_c/u_y2	150	-21%	2
γ100_α_c6_u_c/u_y6	100	-6%	6	γ150_α_c21_u_c/u_y4	150	-21%	4
γ100_α_c14_u_c/u_y2	100	-14%	2	γ150_α_c21_u_c/u_y6	150	-21%	6
γ100_α_c14_u_c/u_y4	100	-14%	4				

Ground Motion Records

In this study, 80 ground motion records with two horizontal components were utilized. As a search criterion, all the records had magnitudes ranging from 6 to 7.9, and their fault mechanism was identified as strike-slip. The ground motion records were then categorized into four groups based on the local soil conditions at the recording station, each comprising 20 ground motions. The stations in the first group correspond to site class A, with an average shear wave velocity exceeding 750 m/s. The second group includes ground motions with average shear wave velocities between 360 m/s and 750 m/s, corresponding to site class B. The third group consists of ground motions with average shear wave velocities between 180 m/s and 360 m/s, denoted as site class C. The last group, corresponding to site class D in accordance with the USGS classification, encompasses the remaining 20 ground motion records with an average shear wave velocity lower than 180 m/s. Details about the selected ground motions can be found in the study conducted by Borekci et al. [28].

Estimation of Inelastic Displacement Ratio (CR)

IDR is the ratio of IDD (u_i) and elastic displacement demand (u_e). It is expressed as in Eq (1) and shown with C_R.

$$C_R = \frac{u_i}{u_e} \tag{1}$$

C_R is estimated for SDOF systems with constant lateral strength. C_R data has been taken from the study of Borekci et al. [28] and the equation of motion was solved with the Newmark-Beta method considering the SSDPH model. Nonlinear time history analyses were performed for SDOF systems with a viscous damping ratio of 5%. The analyses included various strength reduction factors (R_y = 1.5, 2, 3, 4, 5, 6). Inelastic displacement ratios were determined across a range of 53 natural vibration periods ranging from T = 0.1 s to T = 3 s, with specific intervals defined as follows: T = 0.1:0.02:0.2, 0.22:0.03:1, 1.1:0.1:3. The post-yield stiffness ratio (α_s) was considered at values of 0%, 3%, and 5%. For 160 ground motion records, 6 strength reduction factors (R_y), 53 vibration periods (T), 3 post-yield stiffness (α_s), and 27 different degradation combinations, 4121280 nonlinear time history analyses were conducted. All the considered systems reach collapse capacity with dynamic instability before the energy exhaustion. Chenouda and Ayoub [26] conducted a similar study with this study and suggested a "collapse period" (T_{col}) for the limit of dynamic instability.

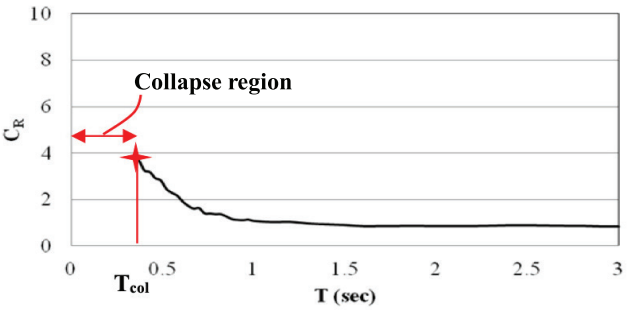

Figure 3. An example for a CR depicting the collapse potential.

In Figure 3, a plot of C_R and limit collapse period is given. A system with a period shorter than the collapse period experiences collapse due to dynamic instability. If more than 50% of the considered ground motion records induce dynamic instability in the structure, it is assumed that a system with this period collapses [26]. To quantify this behavior, a new equation for the collapse period (T_{col}) is proposed. This equation is formulated as a function of degradation parameters (γ, u_c/u_y, α_c), and R_y, and is derived through nonlinear regression analysis. Although Borekci et al. [39] proposed an equation for T_{col} for constant γ (γ = 50,100, 150), the new equation is proposed to estimate T_{col} considering γ when it is needed to use different values of γ except 50, 100, 150 in the estimation of C_R. The proposed equation of T_{col} is given in Eq. (2) and coefficients of Eq. (2) are given in Table 2. It is clear from Table 2 that the correlations of Eq. (2) are considerably high. Detailed information about the estimation of T_{col} can be seen in the study of Borekci et al. [39].

$$T_{col} = 0.1 + x_1 R_y^{x_2} \left(\frac{\left(\frac{u_c}{u_y}\right)^{x_3}}{\alpha_c^{x_4}} + \frac{1}{\gamma^{x_5}} \right) \tag{2}$$

Although C_R is estimated for all systems, C_R values of $T<T_{col}$ are not considered in the estimation of the equation of C_R since it is not logical to determine IDD for the period collapse that occurs. In Figure 4, C_R plots are given for the T = 0 – 3 sec. and T = T_{col} – 3 sec. It is clear from Figure 4, that there is not a useful displacement demand in the collapse zone.

Table 2. Constant parameters of Eq. (2)

Soil Class	x1	x2	x3	x4	x5	R2
A	0.174586	2.009938	-0.7484	-0.677429	0.815143	0.986
B	0.26917	2.36351	-1.2121	-0.94013	0.97244	0.952
C	0.200187	1.760572	-0.6703	-0.782313	0.715947	0.958
D	0.37187	1.72804	-0.608066	-0.734563	0.706503	0.976

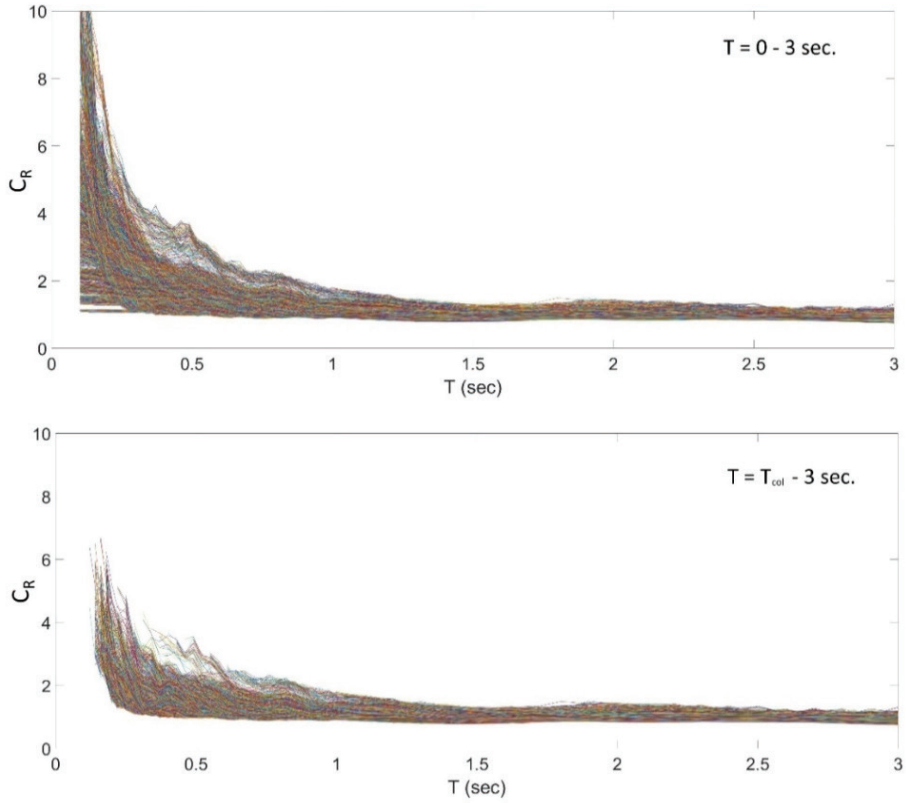

Figure 4. C_R plots estimated via time history analysis.

Borekci et al. [28] proposed an equation for C_R and it is given in Eq. (3). In Eq. (3), a, b, c, d, e, and f are the constants of the equation. Detailed information can be found in the study of Borekci et al. [28].

$$C_R = 1 + a\frac{(R-1)^b}{T^c}\left(\frac{\left(\frac{u_c}{u_y}\right)^d}{(\alpha_c)^e} + \left(\frac{1}{\gamma^f}\right)\right) \quad (3)$$

In this study, C_R values determined in the study of Borekci et al. [28] were estimated via the ANN method and compared with Eq. (3). The flowchart of the MATLAB code for the calculation of C_R is given in Figure 5. System data (R_y, T, γ, u_c/u_y, α_c, α_s) is selected and input into the MATLAB program. T_{col} is estimated with Eq (2) and the period of the system (T) compared with T_{col}. If $T > T_{col}$, C_R is estimated using ANN, else if the program does not estimate C_R since the system collapses.

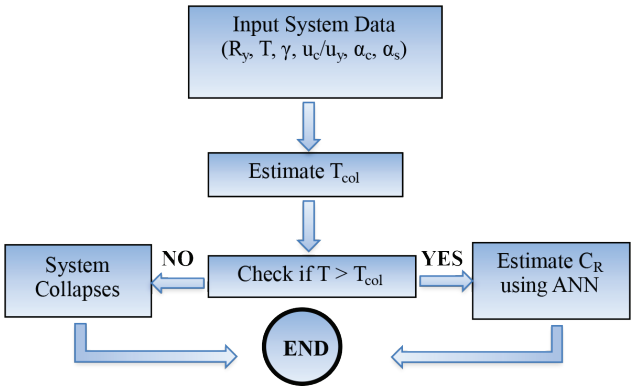

Figure 5. Flowchart for estimating CR employing ANN.

ANN METHODOLOGY

Artificial Neural Network is a commonly used technique, which mimics the neural system of the human brain to solve engineering problems. ANN is a powerful tool, especially for complex engineering problems where the relations among the effective parameters of the problem are difficult to define deterministically. There are different kinds of ANN architectures, but this study is focused on feed-forward back propagation architecture which is one of the most common techniques used in supervised learning. An ANN model has a three-layered fully connected structure consisting of an input layer, hidden layers, and an output layer. Fully connected means that each neuron in a layer is connected to each neuron of the next layer. Thus, the number of connections or synapses between two layers can be calculated by multiplying the number of neurons in two consecutive layers. Each synapse has a weight that is multiplied by its signal or value. The input layer includes

the independent variables which are connected to the first hidden layer which is connected to another hidden layer or finally an output layer. Each hidden layer consists of one or more artificial neurons. A neuron calculates its output (y) as in Eq. (4) using a predetermined activation function (f) and a bias (b). Usually, a sigmoid function is used as an activation function which needs one argument calculated by adding up signals reaching that neuron with the bias.

$$y_j = f\left(b_j + \sum_{i=1}^{n} w_{ij}x_i\right) \quad (4)$$

Where j is the neuron index, n is the number of connections at the input side, w_{ij} is the weight from input i, and the xi is the value from input i.

Each neuron in the Output layer is connected to a single output so the number of neurons in the output layer is limited by the number of outputs. So, this process where each layer feeds the data to the next layer of neurons is called the feed-forward mechanism. Back propagation is the general name for how the errors are calculated and distributed during the training of the ANN. During the supervised training, an expected value for the inputs is known. Hence an error can be calculated and distributed to the neurons by modifying the weights of the connections and the bias of the neurons. Each feed forward and back propagation pair in the training phase is called an epoch. The training continues until certain criteria are met.

The complexity of a neural network is determined by the number of hidden layers and the number of neurons in the hidden layers which directly change the number of unknowns that are needed to be determined by the training, namely the weights and the biases. Since there is no exact method to choosing a number of layers or number of neurons in each layer trial and error method is usually employed. As a rule of thumb simple is better than complex so the goal is to find the simplest architecture which gives good results with a good ability for generalization. The ability of generalization is the ability of the ANN to give good results to unknown input combinations within the input range. When too many hidden neurons/layers are present, or training was continued for too many epochs the ANN may overlearn the training data set which in return will lose its ability to generalize.

The training aims to minimize the errors between the results and the expected values by updating the weights of the connections and the biases. Training of the ANN in this study was conducted by two different training algorithms, Scaled Conjugate Gradient (SCG) and Bayesian Regularization Backpropagation (BRB). SCG method allows the usage of GPU acceleration during the training process while the BRB method uses only CPU.

The SCG algorithm is in the family of Conjugate Gradient (CG) algorithms which was developed to overcome the slow learning process associated with the gradient descent (GD) algorithm. In CG search for the minimum error is conducted in conjugate directions as given in Eq. (5).

$$w_{i+1} = w_i + \alpha_i p_i \qquad p_{i+1} = e_{i+1} + \beta_i p_i \quad (5)$$

Where pi and p_{i+1} are the conjugate directions, w is the weight matrix e is the error matrix, and α_i and β_i have to be calculated in each iteration. A line search is required in each computationally expensive iteration. SCG overcomes this by calculating the Hessian matrix with the approximation given in Eq. (6).

$$E^{"}(w_i)p_i = \frac{E'(w_i + \sigma_i p_i)E'(w_i)}{\sigma_i} + \lambda_i p_i \quad (6)$$

Where E" and E' are the second and the first derivative of the sum of squared error. P is the search direction, σ and λ are parameters controlling the second derivation approximation and indefiniteness of the Hessian Matrix.

Basic methods like standard back propagation or gradient descent backpropagation etc. have very slow convergence. Faster convergence up to 10 – 100 times can be achieved by Levenberg-Marquardt (LM) algorithm [40].

LM optimization is one of the most popular methods in training ANN models due to its speed and accuracy. The speed advantage is achieved by an approximation of the Hessian matrix. The Hessian matrix can be approximated as shown in Eq. (7) when the performance function consists of the square of the errors;

$$H = J^T J \quad (7)$$

Where J is the Jacobian matrix which consists of the first derivatives of the network errors concerning the weights and biases. The gradient, g can be computed as given in Eq. (8);

$$g = J^T e \quad (8)$$

Where e is a vector of errors. The Jacobian matrix is computed by a back propagation technique since it is much less computationally expensive than computing the Hessian matrix. Hence the LM algorithm calculates optimized values by Eq. (9) starting from random initial weights.

$$w_{i+1} = w_i - (J_i^T J_i + \mu_i I)^{-1} J_i^T e_i \quad (9)$$

In Eq. (9), J is the Jacobian matrix of output errors, I is the identity matrix, and μ is a learning parameter.

Training of the ANN in this study was conducted by the BRB algorithm which is an enhanced version of the LM optimization method with improved generalization properties. In the BRB algorithm, the Bayes' theorem incorporates into the regularization scheme. This overcomes some problems like overlearning due to using a high number of neurons or poor learning due to a low number of neurons. BRB algorithm can be defined by the Eq. (10);

$$F(w) = \beta E_D + \alpha E_w\ ;\ E_D = \frac{1}{n}\sum_{i=1}^{n}(o_i^2 - t_i^2)^2\ ;\ E_w = \sum_{i=1}^{m} w_i^2 \quad (10)$$

Where w is the weight, β and α are called regularization parameters, E_w is the sum of squares of network weights, and m is the number of weights. E_w is also known as "penalty term" or "weight decay" or "decay rate". E_D is the error function and is used as the mean of squares of the network error in this study. n is the number of data pairs, o is the prediction from the ANN model and t is the corresponding target value.

In the BRB technique, the uncertainty in the weight vector is taken into account by the probability distribution of beliefs in different values (P(w|α)) which is also called the prior density. During the training process, prior density is converted to a posterior distribution by Bayes' theorem (Eq. (11)).

$$(w|\alpha,\beta,D) = \frac{P(D|w,\beta)P(w|\alpha)}{P(D|\alpha,\beta)} \tag{11}$$

Where P(w|α,β,D) is the posterior density, P(D|w,β) is the likelihood function which is the probability of the error, P(D|α,β) is the evidence or the normalization factor [41].

Maximizing the posterior probability provides the optimal weights of the network in the training process. This can be achieved by minimizing the regularized objective function (F(w)).

Prior and likelihood probabilities can be written as shown in Eq. (12), and Eq. (13), respectively assuming Gaussian distribution for the weight and data.

$$P(w|\alpha) = \frac{1}{Z_w(\alpha)}\exp\left(-\alpha E_w\right) \tag{12}$$

$$P(D|w,\beta) = \frac{1}{Z_D(\beta)}\exp(-\beta E_D) \tag{13}$$

Hence posterior density can be obtained as given in Eq. (14),

$$P(w|\alpha,\beta,D) = \frac{1}{Z_s(\alpha,\beta)}exp\left(-F(w)\right) \tag{14}$$

Then the optimal values of the regularization parameters can be calculated from the data by using Bayes' theorem as shown in Eq. (15),

$$P(\alpha,\beta|D) = \frac{P(D|\alpha,\beta)P(\alpha,\beta)}{P(D)} \tag{15}$$

Where P(α,β)is the prior probability and P(D ├α┤ ,β) is the likelihood term of the regularization parameters [41]. The optimal values of regularization parameters can be obtained by using Eq. (16) [42].

$$\alpha = \frac{\gamma}{2E_w};\ \ \beta = \frac{n-\gamma}{2E_D};\ \gamma = \sum_{i=1}^{m} m - \alpha.trace^{-1}(A) \tag{16}$$

Where γ is the effective parameter, m is the number of parameters, and H is the Hessian matrix of the objective function F(w). Foresee and Hagan [43] described the iterative process for the optimization of the weights and regularization parameters. The procedure starts with the selection of the initial α, β, and w values. Then LM algorithm is run for one epoch to compute the weights which minimize the objective function, F(w). In the next step, γ and the updated values of α and β are computed. Then a new epoch of the LM algorithm is run followed by the update of regularization parameters until convergence is reached.

ANN Structure

Results obtained from the Newmark model were used to train the ANN for the prediction of IDR of degrading SDOF systems. The ANN model has six inputs and one output vector. Input and output vectors are given in Eq. (17) and Eq. (18), respectively. In Eq. (17), St describes the soil type.

$$Input = \left\{S_t, R_y, T, \alpha_c, \gamma, \frac{u_c}{u_y}, \alpha_s\right\} \tag{17}$$

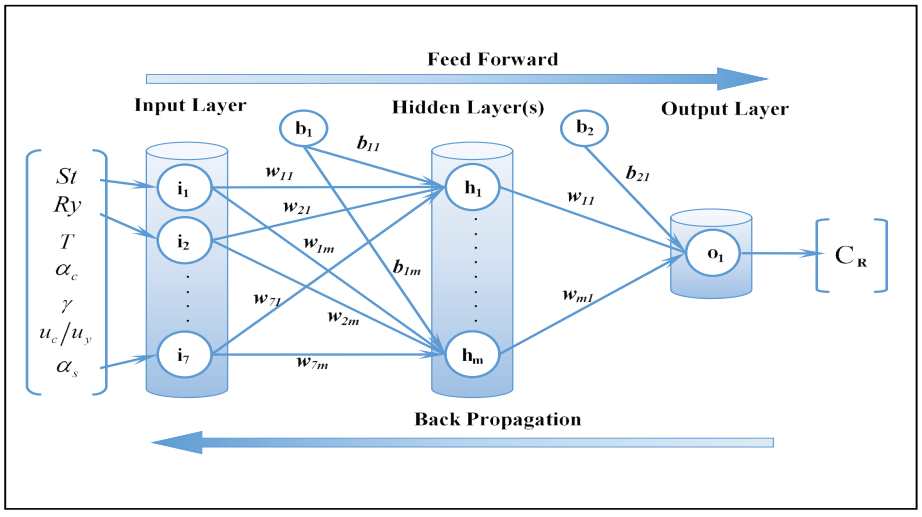

Figure 6. ANN model architecture

$$Output = \{C_R\} \tag{18}$$

Model Architecture showing model inputs and outputs together with model structure is presented in Figure 6. In this study data from 74181 cases were divided into training and validation data sets, %85 of the data was reserved for training while %15 of the data was used for validation to check for overfitting. The check was done by calculating the performance function in the validation data set and stop at the point where the errors in the validation data set continuously increase for a certain number of epochs. When this happens the weights and biases were reverted to the point where the errors were minimum.

ANN model performance was evaluated by using accuracy measures consisting of absolute percentage Error E, Correlation Coefficient (R), Mean Squared Error (MSE) which was also used in the training process, and Mean Absolute Error (MAE). Accuracy measures used in this study are given in Eq. (19) – (22), respectively;

$$E = \frac{|o_i - t_i|}{t_i} \text{x100} \tag{19}$$

$$R = \frac{\sum_{i=1}^{N}(o_i - \bar{o}_i)(t_i - \bar{t}_i)}{\sqrt{\sum_{i=1}^{N}(o_i - \bar{o}_i)^2 \sum_{i=1}^{N}(t_i - \bar{t}_i)^2}} \tag{20}$$

$$MSE = \frac{1}{N}\sum_{i=1}^{N}(t_i - o_i)^2 \tag{21}$$

$$MAE = \frac{1}{N}\sum_{i=1}^{N}|o_i - t_i| \tag{22}$$

Where o_i is the output and t_i is the target value for the i_{th} output. $\overline{o}_i$ is the mean of the output values, and $\overline{t}_i$ is the mean of the target values. N is the number of data pairs.

Optimum Model Selection

All the ANN models created have 7 inputs and one output as described earlier. So, each model searches for the optimum 8-dimensional surface passing through the point cloud. The complexity of the surface is dependent on the number of neurons and the number of hidden layers as they determine the number of parameters to be determined to define the resultant surface. If we define the complexity as the number of unknown parameters to be determined by training, then the complexity of an ANN can be calculated by the following equation.

$$C = \sum_{i=1}^{n-1}(N_i + 1)xN_{i+1} \tag{23}$$

Where n is the number of layers including input and output layers, and N_i is the number of neurons in layer i. The evolution of model performance with model complexity is shown in Figure 7 for different model architectures.

Results show that two and three-layer models converge much faster than the others while giving the best performance per complexity. ANN modeling is not always about getting the minimum error from the model. We also want to have a model with minimum complexity so that the model behavior is more predictable and has a high generalization ability. Up to three hidden layers were considered in this study for both SCG and BRB models. Overall BRB method resulted in higher precision models for one, two, or three hidden layers. An increasing number of hidden layers also increased the accuracy for both SCG and BRB methods. An increasing number of neurons seem to close the error gap between one two and three-layer BRB models. SCG models with higher hidden layer counts usually gave better results than their similar complexity variants with fewer hidden layers.

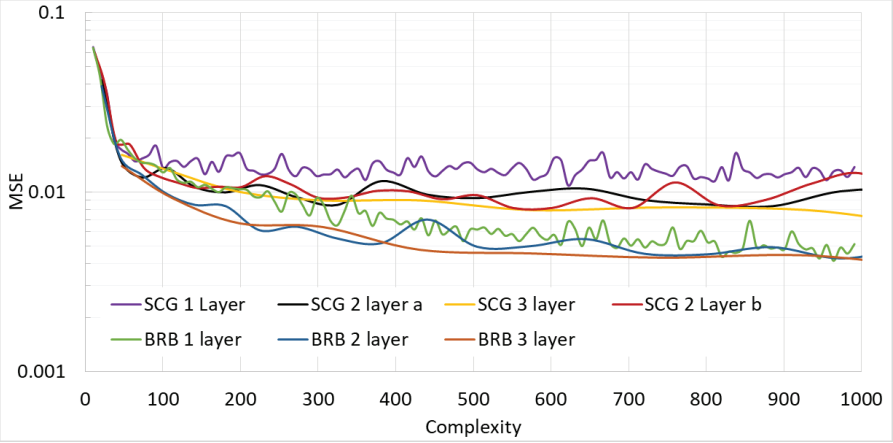

Figure 7. Mean square error of SCG and BRB methods for different model architectures.

COMPARISONS THE RESULTS FOR ANN AND NONLINEAR REGRESSION ANALYSIS

In this study, ANN models for C_R are proposed for degraded peak-oriented hysteretic behavior by BRB and SCG training technique and are compared to nonlinear regression analysis results from Borekci et al. [28]. Although nonlinear regression analysis is a classical method used in literature and many studies use this method to achieve the equation of C_R, ANN is a modern method and almost there is no study about C_R using ANN. This study aims to investigate the reliability and performance of ANN models with

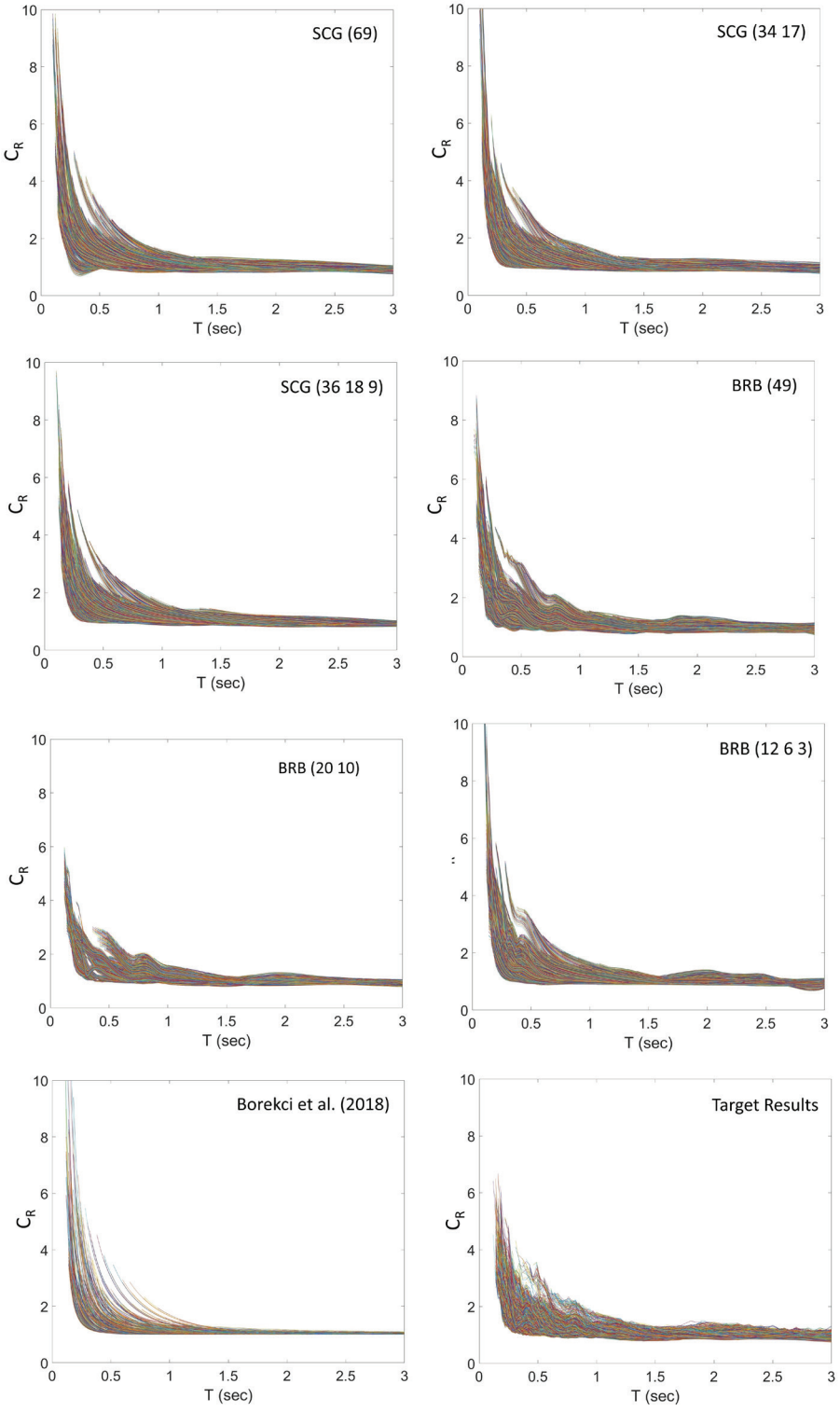

Figure 8. C_R plots for ANN methods, Eq. (3) and exact result architectures.

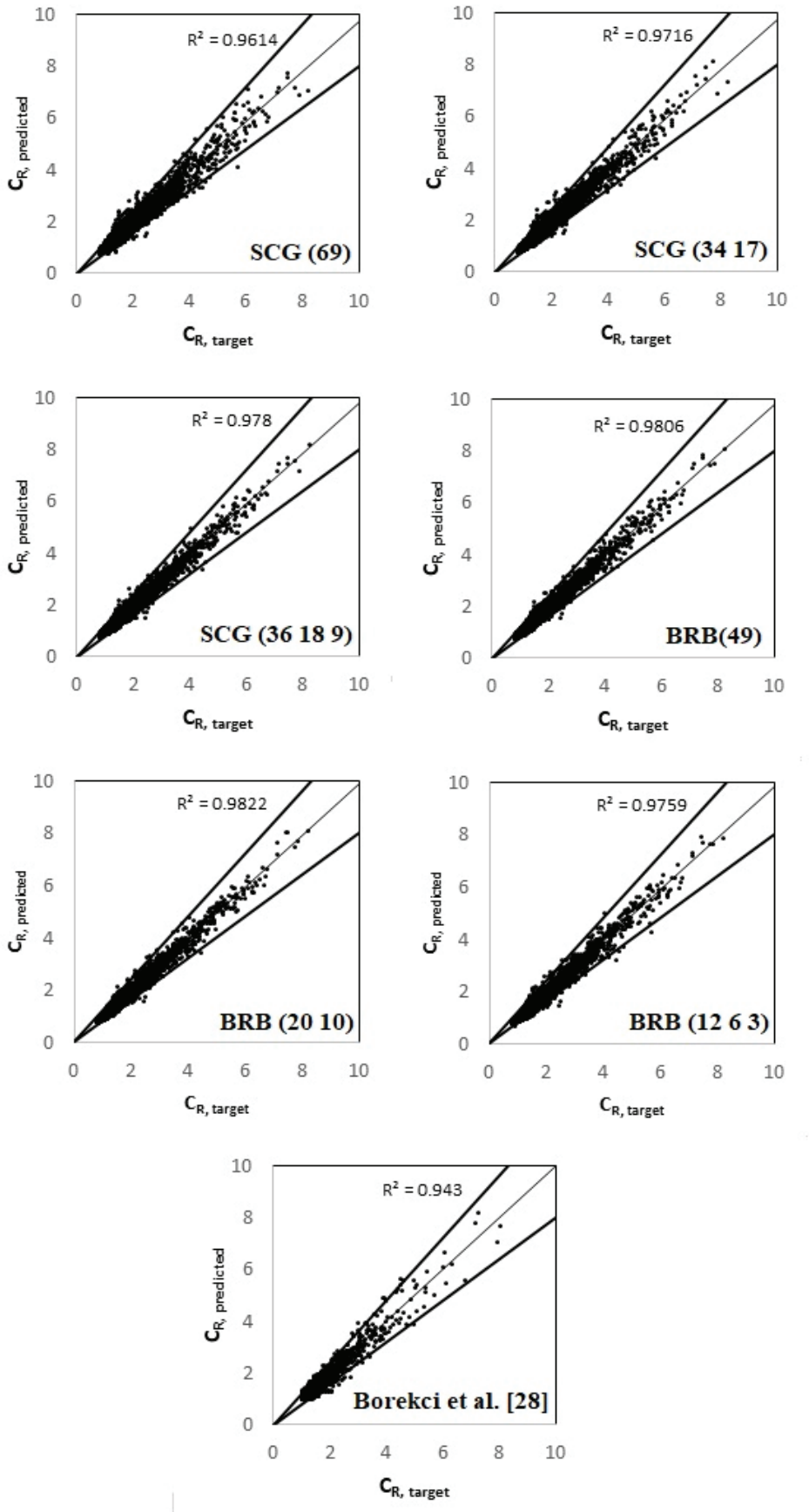

Figure 9. Dispersion of C_R for ANN methods (SCG and BRB) and proposed equation.

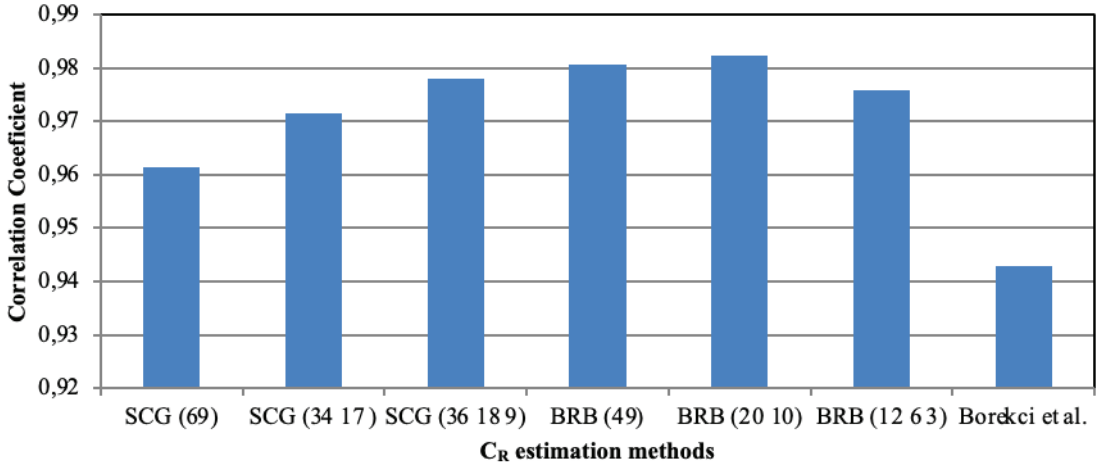

Figure 10. Correlation coefficients of different CR estimation methods.

two different training algorithms and different architectures for the estimation of C_R. In Figure 8, some example C_R plots are given for ANN models, Eq. (3), and the target values. Model names represent the number of neurons in the hidden layers. According to Figure 8, ANN methods give more similar plots to exact results than Eq. (3). Especially, the results of BRB have a good fit with the target results in comparison to SCG. C_R plot of Eq. (3) is very smooth and this smooth behavior is not able to catch the undulations of the target values. A comparison of SCG and BRB shows that SCG models in general have smoother diagrams suggesting that the final values of weights are less than that of similar BRB models.

Scatter diagrams of C_R for ANN methods (SCG and BRB) and Eq. (3) are given in Figure 9. Figure 9 gives the ±20% zone of dispersion. Figure 10 shows the diagram of correlation coefficients of C_R for different estimation methods. According to Figure 9 and Figure 10, the correlation coefficients of all ANN methods are higher than Eq. (3) by Borekci et al. [28]. That means ANN gives more reliable results than nonlinear regression analysis. BRB (20 10) gives the highest correlation coefficient with 0.9822 whereas the Eq. (3) gives the lowest correlation coefficient with 0.943.

The most important thing to keep in mind while using the ANN technique to define a function is the function's validity range. Any function's validity created by ANN curve fitting is limited by the training dataset limits. In this study, the limits of the training dataset are defined by $T_{min} = T_{col}$ value. As a result, the resultant models are only valid between $T=T_{col}$ and T=3 seconds. The lack of points outside the validity range results in unpredictable behavior mostly governed by the points near the edge of the point cloud. Especially models with higher weight values have a higher unpredictability in this region.

CONCLUSION

It is important to determine a reliable IDD in earthquake engineering and C_R is an easy and practical method to estimate IDD. Thus, C_R was estimated for SSDPH behavior with collapse potential to consider the more realistic behavior of RC buildings. In this study, the C_R equation was estimated using ANN methods for the data considered in the study of Borekci et al. [28] and compared with the equation estimated with nonlinear regression analysis. With this study, ANN results of C_R can be given as computer code and researchers and/or engineers can easily estimate more reliable C_R by using this computer code. The following conclusions can be drawn from the results of this study:

- ANN models give better-performing results than the nonlinear regression model in terms of the correlation coefficient. The highest prediction accuracy has been achieved by BRB (20 10) with $R^2 = 0.9822$ correlation coefficient. Even the smallest correlation coefficient of the ANN model, which is 0.9614 of SCG (69), is higher than the coefficient of nonlinear regression analysis with 0.943.
- Despite its complexity, ANN performs better accuracy than nonlinear regression analysis in case of complex relationships between variables. Thus, ANN can be preferred in the prediction of C_R since C_R is susceptible to many variables including structural and ground motion parameters.
- Curve fitting for multi-parameter regression analysis is strongly dependent on the selected formulation. By using ANN, a preselected form is not required.
- SCG ANN models with two and three hidden layers performed better than their one and two hidden layer counterparts.
- SCG ANN models resulted in smoother and less performing results than BRB ANN models.

- BRB ANN models had a steeper learning curve achieving better performance with less complexity. Also, two and three hidden layer BRB models achieved similar performance levels but achieved better than single layer BRB models at low complexity. As the complexity increases the difference in model performance between single and more hidden layer models was decreased.
- ANN models will give a continuous space of results. When the output space is limited by a combination of input parameters, some criteria are needed to be adopted to eliminate results outside the valid range. A new T_{col} equation is proposed to use with the ANN model.

As a result, ANN performs better accuracy in the prediction of C_R than the nonlinear regression model. It is recommended to use the proposed ANN model to estimate a reliable inelastic displacement ratio of degrading RC structures. Since it may help in the selection of proper records in the C_R estimation procedure, it can be important to evaluate the effects of each ground motion parameter on C_R, taking into account the soil-structure interaction, in future studies.

AUTHORSHIP CONTRIBUTIONS

Authors equally contributed to this work.

DATA AVAILABILITY STATMENT

The authors confirm that the data that supports the findings of this study are available within the article. Raw data that support the finding of this study are available from the corresponding author, upon reasonable request.

CONFLICT OF INTEREST

The author declared no potential conflicts of interest with respect to the research, authorship, and/or publication of this article.

ETHICS

There are no ethical issues with the publication of this manuscript.

REFERENCES

[1] Newmark NM. Effect of inelastic behavior on the response of simple systems to earthquake motions. In: Proceedings of the 2nd World Conference on Earthquake Engineering; 1960; Tokyo, Japan. p. 895–912.

[2] Shimazaki K, Sozen MA. Seismic drift of reinforced concrete structures. Tokyo: Hazama-gumi; 1984.

[3] Qi X, Moehle JP. Displacement design approach for reinforced concrete structures subjected to earthquakes. Berkeley (CA): Earthquake Engineering Research Center, College of Engineering, University of California; 1991.

[4] Miranda E. Seismic evaluation and upgrading of existing structures [Dissertation Thesis]. Berkeley (CA): University of California; 1991.

[5] Miranda E. Evaluation of seismic design criteria for highway bridges. Earthquake Spectra 1993;9:233–250. [CrossRef]

[6] Miranda E. Evaluation of site-dependent inelastic seismic design spectra. J Struct Eng 1993;119:1319–1338. [CrossRef]

[7] Miranda E. Inelastic displacement ratios for structures on firm sites. J Struct Eng 2000;126(10):1150–1159. [CrossRef]

[8] Ruiz-García J, Miranda E. Inelastic displacement ratios for evaluation of existing structures. Earthquake Eng Struct Dyn 2003;32:1237–1258. [CrossRef]

[9] Vidic T, Fajfar P, Fischinger M. Consistent inelastic design spectra: strength and displacement. Earthquake Eng Struct Dyn 1994;23:507–521. [CrossRef]

[10] Aydinoglu MN, Kacmaz U. Strength-based displacement amplification spectra for inelastic seismic performance evaluation. Istanbul: Bogazici University, Department of Earthquake Engineering; 2002 Report No.: 2002/2.

[11] Chopra AK, Chintanapakdee C. Inelastic deformation ratios for design and evaluation of structures: single-degree-of-freedom bilinear systems. J Struct Eng 2004;130:1309–1319. [CrossRef]

[12] Eser M, Aydemir C, Ekiz I. Inelastic displacement ratios for structures with foundation flexibility. KSCE J Civ Eng 2012;16:155–162. [CrossRef]

[13] Durucan C, Durucan AR. Ap/Vp specific inelastic displacement ratio for the seismic response estimation of SDOF structures subjected to sequential near fault pulse type ground motion records. Soil Dyn Earthquake Eng 2016;89:163–170. [CrossRef]

[14] Zhai CH, Wen WP, Zhu TT, Li S, Xie LL. Inelastic displacement ratios for design of structures with constant damage performance. Eng Struct 2013;52:53–63. [CrossRef]

[15] Wen WP, Zhai CH, Li S, Chang Z, Xie LL. Constant damage inelastic displacement ratios for the near-fault pulse-like ground motions. Eng Struct 2014;59:599–607. [CrossRef]

[16] Ibarra LF, Medina RA, Krawinkler H. Hysteretic models that incorporate strength and stiffness deterioration. Earthquake Eng Struct Dyn 2005;34:1489–14511. [CrossRef]

[17] Braz-César MT, Oliveira DV, Barros RC. Comparison of cyclic response of reinforced concrete infilled frames with experimental results. In: Proceedings of the 14th World Conference on Earthquake Engineering; 2008; Beijing, China.

[18] Luo H, Paal SG. Machine learning-based backbone curve model of reinforced concrete columns subjected to cyclic loading reversals. J Comput Civ Eng 2018;32:04018042. [CrossRef]

[19] Chintanapakdee C, Jaiyong A. Estimation of peak roof displacement of degrading structures. In: Proceedings of the 15th World Conference on Earthquake Engineering; 2012; Lisbon, Portugal.
[20] Nassar AA. Seismic demands for SDOF and MDOF systems [thesis]. Stanford (CA): Stanford University; 1991.
[21] Rahnama M, Krawinkler H. Effects of soft soils and hysteresis models on seismic design spectra. Stanford (CA): John A. Blume Earthquake Engineering Center, Stanford University; 1993. Report No.: 107.
[22] Seneviretna GDPK, Krawinkler H. Evaluation of inelastic MDOF effects for seismic design. Stanford (CA): John A. Blume Earthquake Engineering Center, Stanford University; 1997. Report No.: 120.
[23] Gupta B, Kunnath SK. Effect of hysteretic model parameters on inelastic seismic demands. In: Proceedings of the 6th US National Conference on Earthquake Engineering; 1998 May; Seattle, WA. p. 1-12.
[24] Song JK, Pincheira JA. Spectral displacement demands of stiffness-and strength-degrading systems. Earthquake Spectra 2000;16:817–851. [CrossRef]
[25] Pekoz HA, Pincheira JA. Seismic Response of Strength and Stiffness Degrading Single Degree of Freedom Systems. In: Proceedings of the 13th World Conference on Earthquake Engineering; 2004 Aug 1-6; Vancouver, BC, Canada.
[26] Chenouda M, Ayoub A. Inelastic displacement ratios of degrading systems. J Struct Eng 2008;134:1030–1045. [CrossRef]
[27] Lumantarna E, Lam N, Wilson J, Griffith M. Inelastic displacement demand of strength-degraded structures. J Earthquake Eng 2010;14:487–511. [CrossRef]
[28] Borekci M, Kırçıl MS, Ekiz I. Inelastic displacement ratios for evaluation of degrading peak-oriented SDOF systems. Period Polytech Civ Eng 2018;62:33–47. [CrossRef]
[29] Xie Y, Ebad Sichani M, Padgett JE, DesRoches R. The promise of implementing machine learning in earthquake engineering: A state-of-the-art review. Earthquake Spectra 2020;36:1769–1801. [CrossRef]
[30] Dwairi HM, Tarawneh AN. Artificial neural networks prediction of inelastic displacement demands for structures built on soft soils. Innov Infrastruct Solut 2022;7:4. [CrossRef]
[31] Wei M, Hu X, Yuan H. Residual displacement estimation of the bilinear SDOF systems under the near-fault ground motions using the BP neural network. Adv Struct Eng 2022;25:552–571. [CrossRef]
[32] Clough RW. Effect of stiffness degradation on earthquake ductility requirements. In: Proceedings of the Japan Earthquake Engineering Symposium; 1966.
[33] Mahin SA, Bertero VV. An evaluation of some methods for predicting seismic behavior of reinforced concrete buildings. Berkeley (CA): University of California, Earthquake Engineering Research Center; 1975.
[34] Ibarra LF. Global collapse of frame structures under seismic excitations [thesis]. Stanford (CA): Stanford University; 2004.
[35] Miranda E, Akkar SD. Dynamic instability of simple structural systems. J Struct Eng 2003;129(12):1722–1726. [CrossRef]
[36] Ayoub A, Chenouda M. Response spectra of degrading structural systems. Eng Struct 2009;31:1393–1402. [CrossRef]
[37] Bernal D. Instability of buildings during seismic response. Eng Struct 1998;20:496–502. [CrossRef]
[38] Villaverde R. Methods to assess the seismic collapse capacity of building structures: State of the art. J Struct Eng 2007;133:57–66. [CrossRef]
[39] Borekci M, Kirçil MS, Ekiz I. Collapse period of degrading SDOF systems. Earthquake Eng Eng Vib 2014;13:681–694. [CrossRef]
[40] Hagan MT, Menhaj MB. Training feedforward networks with the Marquardt algorithm. IEEE Trans Neural Netw 1994;5:989–993. [CrossRef]
[41] MacKay DJC. Bayesian model comparison and backprop nets. In: Advances in Neural Information Processing Systems 4. 1991.
[42] Burden F, Winkler D. Bayesian regularization of neural networks. In: Artificial Neural Networks: Methods and Applications. 2009. p. 23–42. [CrossRef]
[43] Foresee FD, Hagan MT. Gauss-Newton approximation to Bayesian learning. In: Proceedings of the International Conference on Neural Networks (ICNN'97); 1997 Jun 12; Houston, TX. IEEE. vol. 3, p. 1930–1935.